Micro and Nano Systems Letters

LETTER Open Access

Copper micromesh-based lightweight transparent conductor with short response time for wearable heaters

Han-Jung Kim and Yoonkap Kim*

Abstract

Thickness-controlled transparent conducting films (TCFs) were fabricated by transfer printing a 100 nm thick Cu micromesh structure onto poly(vinyl alcohol) (PVA) substrates of different thicknesses (~ 50, ~ 80, and ~ 120 μm) to develop a lightweight transparent wearable heater with short response time. The Cu mesh-based TCF fabricated on a ~ 50 μm thick PVA substrate exhibited excellent optical and electrical properties with a light transmittance of 86.7% at 550 nm, sheet resistance of ~ 10.8 Ω/sq, and figure-of-merit of approximately 236, which are comparable to commercial indium tin oxide film-based transparent conductors. The remarkable flexibility of the Cu mesh-based TCF was demonstrated through cyclic mechanical bending tests. In addition, the Cu mesh-based TCF with ~ 50 μm thick PVA substrate demonstrated a fast Joule heating performance with a thermal response time of ~ 18.0 s and a ramping rate of ~ 3.0 ℃/s under a driving voltage of 2.5 V. Lastly, the reliable response and recovery characteristics of the Cu mesh/PVA film-based transparent heater were confirmed through the cyclic power test. We believe that the results of this study is useful in the development of flexible transparent heaters, including lightweight deicing/defogging films, wearable sensors/actuators, and medical thermotherapy pads.

Keywords: Wearable transparent heater, Transparent conductor, Metal mesh, Thermal response time, Transfer printing

Introduction

Transparent heaters (THs) have been studied for multiple potential applications, including smart windows [1, 2], defrosters [3, 4], thermochromic displays [5, 6], physical/chemical sensors [7, 8], and other advanced heat-generating systems [9–11]. High optical transparency and excellent electrical conductivity are two important factors for high-performance THs. Moreover, this technology is being mainly developed based on the research results of existing transparent conductors with transparent conductive oxides (TCOs), such as indium tin oxide (ITO) and fluorine-doped tin oxide (FTO) films [12]. However, owing to their brittle nature, it is extremely difficult to adapt TCO films in the development of next-generation transparent conductors for flexible/wearable TH applications [11]. Thus, there has been active research on the replacement of commercial TCO films for flexible/wearable THs.

The potential candidate materials for ITO/FTO-free flexible/wearable THs include conductive polymers [6], carbon-based nanomaterials [5, 13, 14], metal-based nano/micro-materials [3, 4], and other hybrid materials [15, 16]. Conductive polymers, such as poly(3,4-ethylen edioxythiophene):poly(styrene sulfonate) (PEDOT:PSS), have outstanding advantages in terms of mechanical flexibility and solution processibility; however, conductive polymers have low electrical conductivity, and poor stability against heat and moisture, thereby limiting their application in high-performance optoelectronic devices

*Correspondence: yoonkap@geri.re.kr
Convergence Materials Research Center, Gumi Electronics and Information Technology Research Institute (GERI), Cheomdangieop 1-ro, Sandong-myeon, Gumi 39171, Gyeongbuk, Korea

[17, 18]. Meanwhile, carbon nanomaterials, such as graphene and carbon nanotubes, have excellent thermal conductivity and flexibility; however, the manufacturing costs for high-quality carbon-based nanomaterials through thermal and plasma chemical vapor deposition techniques are usually expensive [11, 19]. Accordingly, owing to their relatively simple manufacturing process (high productivity) and superior physical properties, such as optical/electrical conductance and mechanical flexibility, the development of metal-based flexible THs with metal nanowires (NWs) and mesh structures have recently garnered considerable attention as an alternative to commercial TCO films [3, 4, 9, 20]. Park et al. proposed a stretchable TH with a stable operation at ~ 250 ℃ using Ag nanofibers on transparent polyimide film, which can be applied to wearable heaters [21]. Ko et al. also reported a stretchable TH using Ag NWs on polydimethylsiloxane substrate with stable operation at ~ 60 ℃, which has potential applications in wearable electronics [22]. Cui et al. reported a flexible TH using printed Cu mesh on polyethylene terephthalate substrate with stable operation at ~ 110 ℃ for automotive windshield heating film application [23]. Thus, there has been various research on the fabrication and performance of flexible/wearable THs based on micro/nano-scale metal materials. Nevertheless, the development of wearable ITO/FTO-free THs with faster response characteristics needs to be further investigated.

In this study, we introduce a new strategy to develop a lightweight flexible TH with short response time for wearable thermotherapy and heating systems. A 100 nm thick conductive Cu mesh structure with optically transparency and electrically conductivity was fabricated onto poly(vinyl alcohol) (PVA) substratses of different thicknesses (~ 50, ~ 80, and ~ 120 μm) through transfer printing method. A lightweight flexible Cu mehs/PVA film-based transparent conducting film (TCF) based on a ~ 50 μm thick PVA substrate with optical and electrical properties comparable to commercial ITO glass was sucessfully fabricated. Further, the Cu mesh/PVA film-based TCF demonstrated its fast, stable, and reliable performance for TH applications. Finally, for its actual application, the Cu mesh/PVA film-based TH was attached to a finger and the back of the hand.

Experimental

Materials

Ultraviolet (UV)-curable polyurethane acrylate (PUA) imprint resin (MINS-311RM) and 99.99% Cu were purchased from Changsung Sheet Co., Ltd. (Korea) and Taewon Scientific Co. Ltd. (Korea), respectively. And, PVA powders (Mw of 85,000–124,000) and trichloro(1*H*,1*H*,2*H*,2*H*-perfluorooctyl)silane (97%) were purchased from Sigma-Aldrich Inc. (USA).

Optical, electrical, and structural characterization

The optical transmittance spectra of the prepared Cu mesh-based TCFs were obtained using a UV–visible near-infrared spectrometer (Cary 5000 UV–vis-NIR, Agilent, USA) with air as the reference. The electrical conductance (sheet resistance) of the Cu mesh-based TCF was measured using a four-point probe method with a sheet resistivity meter (FPP-2000, DASOL ENG, Korea). The TH structure was analyzed using a field-emission scanning electron microscope (FE-SEM, Sirion, FEI, USA) and optical microscope (BX51, OLYMPUS, Japan). The weight of the fabricated felxible TCFs were measured using a precision electronic balance (HM-202, A&D Co. Ltd, Japan). The sheet resistance, optical transmittance, and weight of the TCF were measured at least five times, and then the average value was taken.

Evaluation of the electrothermal performance of the Cu mesh-based TCFs

To investigate the Joule heating performance of the Cu mesh-based TCF, direct current (DC) voltages of 0.5, 1.0, 1.5, 2.0, and 2.5 V was applied to the TCF through contact with the Ag side. The resulting temperature change was recorded by a direct measurement using a thermocouple (ST-50, RKC Instrument Inc., Japan) mounted on the PVA substrate part without a Cu mesh. The temperature on the surface of the TH was measured three times and the average value was used. The obtained temperature profile was confirmed using an infrared (IR) camera (Seek Compact, Seek Thermal Inc., USA).

Results and discussion

In this work, TCFs based on a uniform Cu mesh structure were fabricated by a tranfer printing method without a lift-off, etching or electroplating process [24]. First, a PUA mold with an engraved micromesh pattern was replicated from a silicon master through a replicate molding method (see Additional file 1: Figure S1). Here, the silicon master used in this work could be prepared by photolithography and dry etching techniques. The surface of the PUA mold was treated with a layer of 1*H*,1*H*,2*H*,2*H*-perfluorooctyl-trichlorosilane to form an anti-sticking layer covering. A thin Cu layer with a thickness of 100 nm was deposited on the surface of the PUA mold using an electron-beam evaporator, as shown in Fig. 1a. For this step, Cu has an evaporation rate of approximately 0.1 nm/s. Here, the Cu layer deposited on the PUA mold with the anti-sticking layer was designed to be easily peeled off. A transparent PVA substrate was used as the receiver for the selective transfer of the Cu mesh layer from the PUA

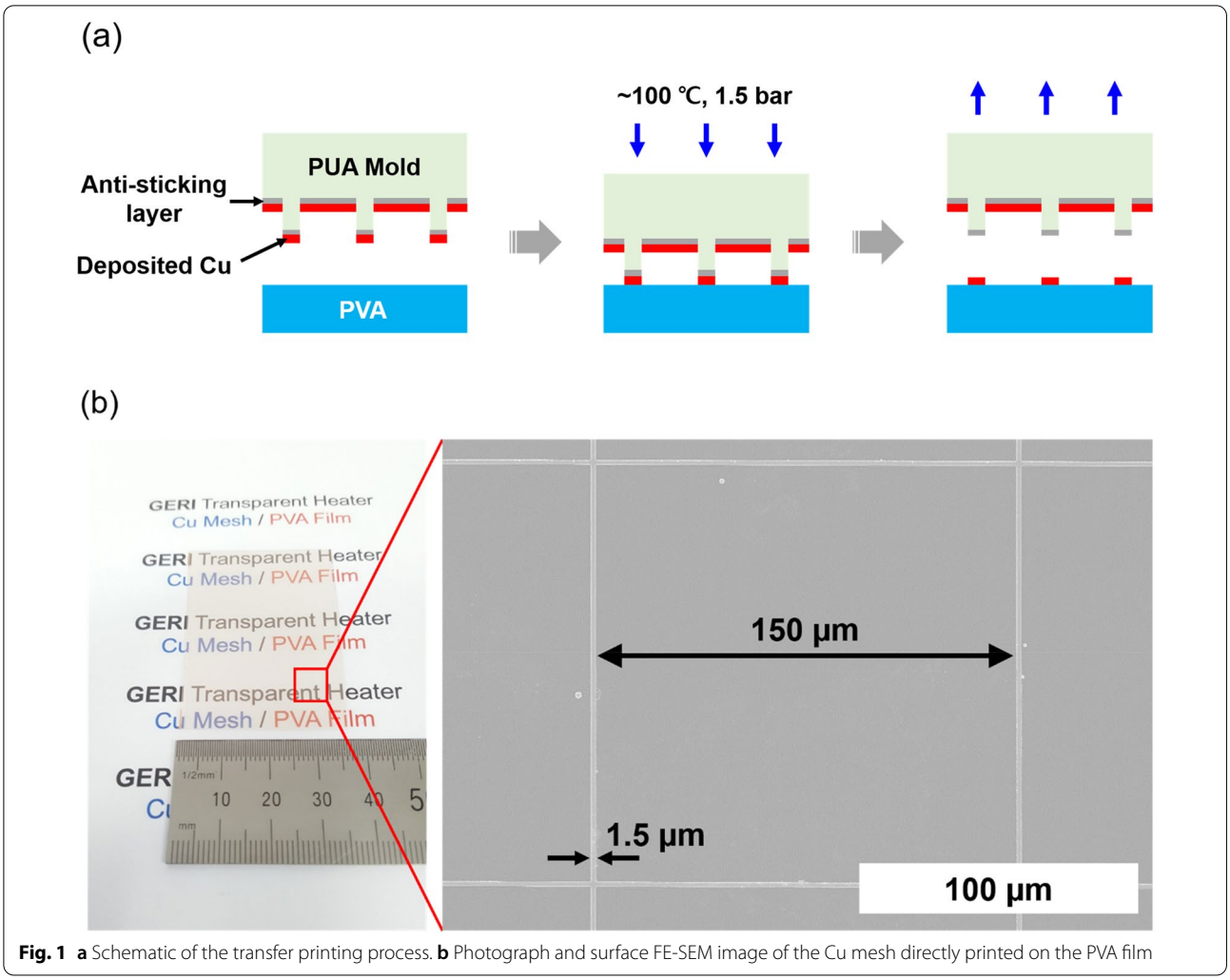

Fig. 1 **a** Schematic of the transfer printing process. **b** Photograph and surface FE-SEM image of the Cu mesh directly printed on the PVA film

mold to fabricate the TH substrate. A 20 wt.% aqueous PVA solution with viscosity of ~ 20,000 cP was bar-coated onto a cleaned glass plate and cured in a drying oven at 50 ℃ for 24 h, thereby a PVA film with constant thickness was obtained by controlling the gap between the glass plate and blade. After thermal curing, the PVA film was carefully separated from the glass plate. The Cu thin film-deposited PUA mold was then placed in contact with the surface of the PVA film. The PUA mold/PVA film was assembled through hot-pressing by applying ~ 1.5 bar static pressure at ~ 100 ℃ for 3 min. Subsequently, the PUA mold/PVA film was naturally cooled to room temperature (RT). Finally, a uniform Cu mesh structure on the PVA film was obtained after peeling the PUA mold. Figure 1b shows a photograph and surface FE-SEM image of the Cu mesh structure printed on the PVA film. Additional file 1: Figure S2 shows an optical microscope image of the Cu mesh/PVA film surface observed at a low magnification. A Cu mesh structure with a line width of 1.5 μm and a line spacing of 150 μm was sucessfully formed on the PVA film. Further, the optical transparency of the Cu mesh/PVA film is confirmed.

Figure 2 shows the performance of the Cu mesh/PVA film as a transparent conductor. As shown in Fig. 2a, a red light-emitting diode (LED) turned on using the ~ 50 μm thick Cu mesh/PVA film-based TCF. The as-prepared Cu mesh/PVA film-based TCF exhibited an optical transmittance of 86.7% at 550 nm, average transmittance of ~ 85.0% over the entire visible range (see Additional file 1: Figure S3), and average sheet resistance of ~ 10.0 Ω/sq (see Additional file 1: Figure S4). The optical transmittance at 550 nm, sheet resistance, and figure-of-merit (FOM) of the commercial ITO glass and Cu mesh/PVA film-based TCFs with various thicknesses are summarized in Table 1. The FOM value is calculated as the ratio of the electrical conductance (σ_{dc}) to the optical conductance (σ_{opt}), following the equation: [24]

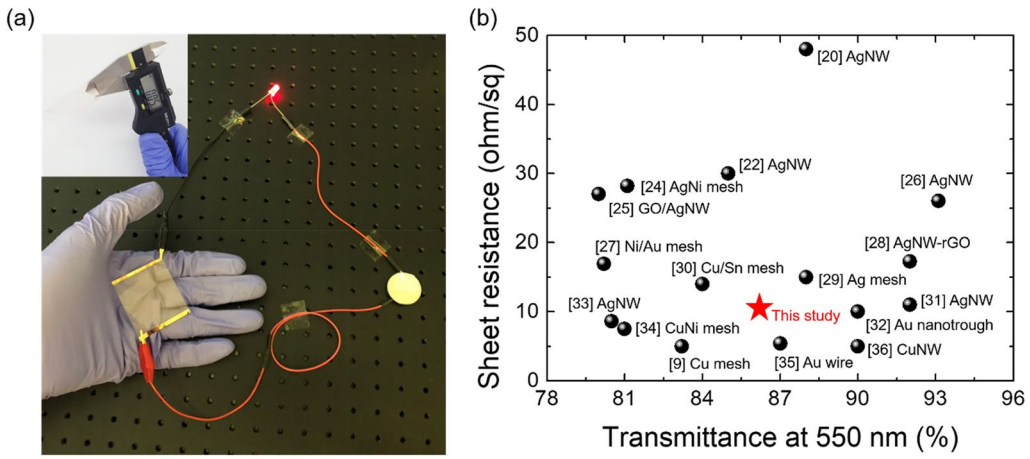

Fig. 2 **a** Digital photograph of the Cu mesh/PVA film (45 mm × 45 mm) with ~ 50 μm thick PVA substrate as a transparent conductor in an electronic circuit connected to a LED. **b** Comparison of the optical transmittance and sheet resistance of the Cu mesh/PVA film with ~ 50 μm thick PVA substrate fabricated this study, and those of previously reported metal-based transparent conductors. The numbers in the square brackets indicate the cited references

Table 1 Transmittance at 550 nm, average sheet resistance, and FOM of the commecial ITO glass and fabricated Cu mesh/PVA films with various substrate thicknesses

Sample	Transmittance at 550 nm (%)	Sheet resistance (ohm/sq)	FOM
~ 50 μm thick Cu mesh/PVA film	86.7	~ 10.8	236.1
~ 80 μm thick Cu mesh/PVA film	86.5		232.0
~ 120 μm thick Cu mesh/PVA film	86.4		230.2
Commercial ITO glass (0.7 mm)	85.6	~ 10.0	235.6

$$\sigma_{dc}/\sigma_{opt} = Z_0/2R_S\left(T^{-1/2}-1\right) \quad (1)$$

where R_S and T are the measured sheet resistance and the optical transmittance at 550 nm, respectively, and Z_0 is the impedance at free space (377 Ω). As shown in the Table 1, the Cu mesh/PVA film with ~ 50 μm thick PVA substrate has an FOM value of 236.1, which is similar to that of commercial ITO glass (235.6). The weights of the Cu mesh-based TCFs fabricated on ~ 50, ~ 80, and ~ 120 μm thick PVA films were measured to be 27.8, 42.7, and 65.9 mg, respectively. The weight per unit area of the Cu mesh-based TCF with ~ 50 μm PVA substrate was approximately 0.0695 mg/mm^2. As seen in Fig. 2b, the optical and electrical conductance of the Cu mesh/PVA film-based TCF with ~ 50 μm thick PVA substrate was comparable to that of other metal-based transparent conductors [9, 20, 22, 24–36].

To apply the fabricated Cu mesh/PVA film-based TCF to flexible/wearable electronic devices, the change in the current–voltage relationship under bending should be investigated. Thus, the current of the Cu mesh/PVA film-based TCF with ~ 50 μm thick PVA substrate was measured with different input voltages with its flat and bent state. As shown in Fig. 3a, the current steadily increased up to 288 mA at an applied voltage of 3.0 V in the flat state. In contrast, when the Cu mesh/PVA film was bent with an outside bending radius of 5 mm, the current slightly decreased to 277 mA at 3.0 V. The slight decrease in the current at a relatively high input voltage range (2.0–3.0 V) is mainly attributed to the decrease in the local connectivity between the evaporated Cu particles induced by the bending stress.

Figure 3b shows the changes in the sheet resistance of the Cu mesh/PVA film and ITO/PVA film-based TCFs fabricated with the same thickness (~ 50 μm) as the bending radius decreases. The sheet resistance of the ITO/PVA film-based TCF with an initial sheet resistance of ~ 30 Ω/sq significantly increased when the bending radii were less than 10 mm due to the increased brittleness of ITO thin film [29]. The cracks formed on the surface of the ITO film could be confirmed after the mechanical bending test, as shown in the optical microscope image inserted in Fig. 3b. In contrast to the ITO/PVA film-based TCF, there were no changes observed in the initial sheet resistance (~ 11 Ω/sq) of the Cu mesh/PVA film-based TCF even at a bending radius as small as 4 mm. Figure 3c shows the changes in the sheet resistance

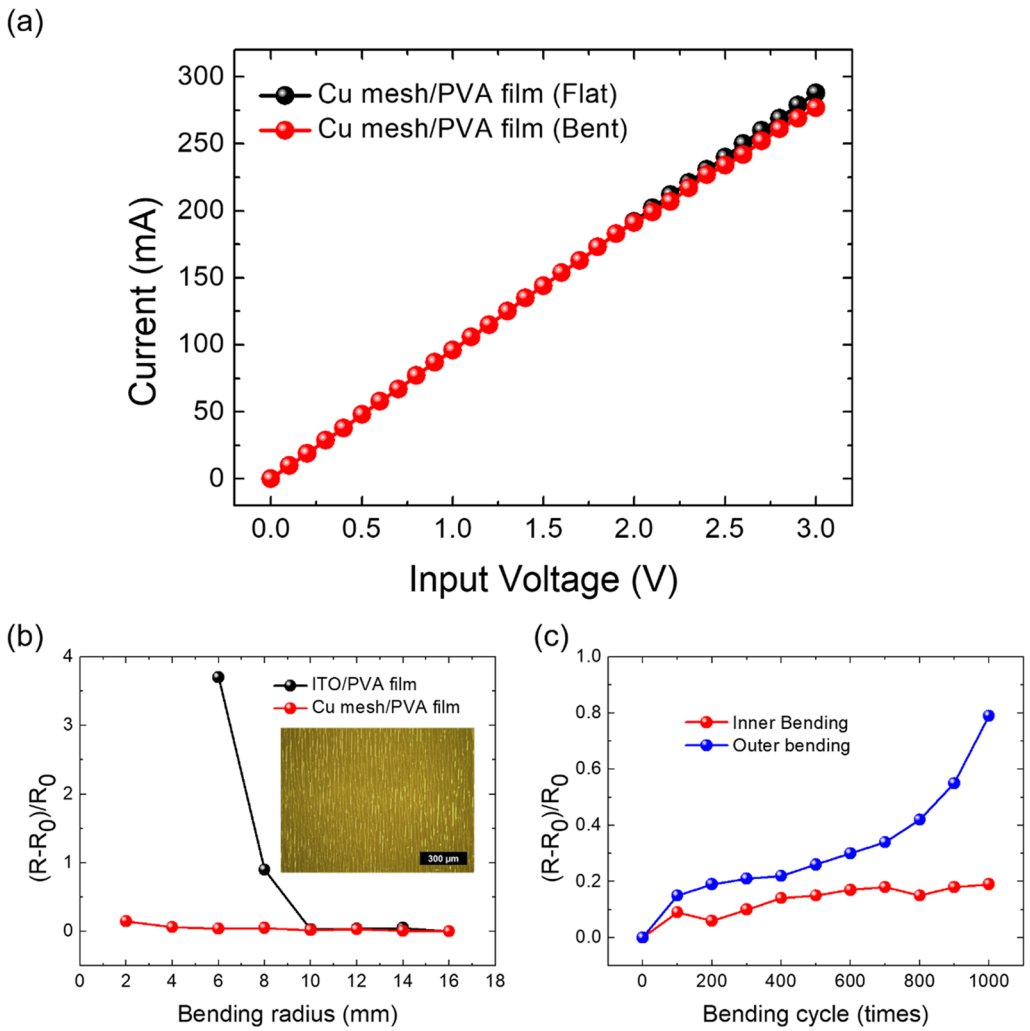

Fig. 3 **a** Current–voltage relationship of Cu mesh/PVA film (45 mm × 45 mm) in its flat and bent state with a bending radius of 5 mm. **b** Changes in the sheet resistance of the Cu mesh/PVA film and ITO/PVA films as a function of the bending radius. The inset shows an optical microscope image of the ITO film after the bending test. **c** Changes in the sheet resistance of the Cu mesh/PVA film with ~ 50 μm thick PVA substrate with respect to the bending cycles at a fixed bending radius of 4 mm

with the increase of the bending cycles for the outward and inward bending fatigue tests of the Cu mesh/PVA film-based TCF with ~ 50 μm thick PVA substrate at a fixed bending radius of 4 mm. After 1,000 cycles, the sheet resistance of the Cu mesh/PVA film-based TCF marginally increased to ~ 20% for the inner bending tests, whereas it increased by ~ 80% for the outer bending tests. These experimental results indicate that the uniform Cu mesh structure is more vulnerable to failure under external bending stress than internal bending stress.

The excellent flexibility of the Cu mesh/PVA film-based TCF was further demonstrated by lighting a red LED using the fabricated Cu mesh/PVA film-based TCF as the flexible transparent conductor, as shown in Fig. 4. Particularly, there are no noticeable changes in the LED brightness before and after bending the TCF.

Figure 5a shows the time-dependent temperature of the Cu mesh/PVA film as a TH with a sheet resistance of ~ 11.0 Ω/sq. By applying different bias voltages (0.5–2.5 V), the temperature of the Cu mesh/PVA film-based TH rapidly increased from RT to saturated values until the thermal equilibrium was achieved. The temperature of the TH rapidly increased with respect to the driving voltage. At a driving voltage of 2.5 V, the temperature of the TH reached ~ 85.0 ℃. The heat generation of the Cu mesh/PVA film-based TH first occurred through Joule heating. The generated heat subsequently dissipated through conduction in the substrate, air convection, and

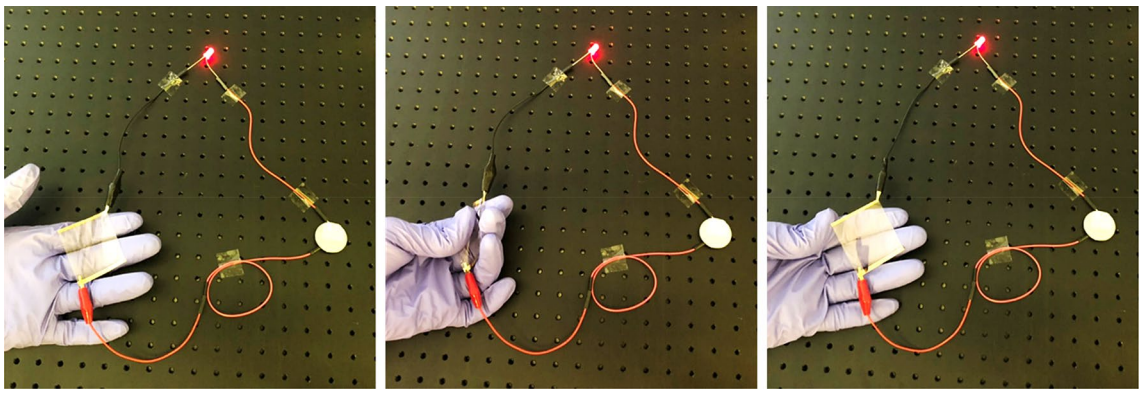

Fig. 4 Photographs of the 45 mm × 45 mm Cu mesh/PVA film used as the transparent electrode to power a red LED before and after manual bending

radiation [9]. When the applied voltage was cut off, the temperature of the TH decreased to RT in ~ 60 s. Figure 5b shows the time–temperature curves of the TH with different PVA film thicknesses at a constant input voltage of 2.5 V. The response time, which is defined as the time required to reach 90% of the steady-state temperature during operation, of the Cu mesh/PVA film-based THs with a PVA film with thickness of ~ 50, ~ 80, and ~ 120 μm were 18.0, 21.5, and 23.5 s, respectively. Here, the average response time of the THs with various PVA film thickness was reproducible with a relative standard deviation of only 2.1%. And, the response time of the TH based on Cu mesh/PVA film with a thickness of ~ 50 μm is much faster than that of the flexible TH reported so far (see Additional file 1: Table S1) [Additional file 1: S1-5, 23, 26]. The thinner Cu mesh/PVA film TH exhibited shorter thermal response time and faster ramp rate (see Table 2). The decrease in the heater response time due to the decrease in the thickness of the heater substrate (PVA film) could be explained as follows. For a Cu mesh/PVA film-based TH at a given driving voltage, the heating (ramping) rate and saturated temperature depend on the thermal properties of the heating element (Cu mesh structure) and the heater substrate (PVA film). Generally, response time is related to the time constant (τ) of the transient thermal response depicted as: [16]

$$\tau = C/hA \tag{2}$$

where C refers to the heat capacity, h is the heat transfer coefficient, and A is the surface area. In this study, the heating element (Cu mesh structure) thickness of ~ 100 nm can be deemed negligible compared to the thickness of the heater substrate (PVA film), which is in the range of 50–120 μm. Therefore, the heat capacity (C) of the Cu mesh structure could be neglected and that of the PVA film dominates the transient process of the electrothermal response. Thus, τ can be rewritten as Eq. (3).

$$\tau = C/hA = cm/hA = \rho dc/h \tag{3}$$

where c, m, ρ, and d are the specific heat capacity, mass, density, and thickness of the PVA film, respectively. Therefore, the response time of the Cu mesh/PVA film-based TH could be reduced by reducing the thickness of the heater substrate (PVA film).

The repeatability of the heat generation of the TH was investigated by a cyclic test of 10 on/off cycles. As shown in Fig. 5c and Table 3, there were no significant changes in the thermal response/recovery characteristics of the Cu mesh/PVA film-based TH during the cyclic test.

Joule heating demonstrated a self-annealing effect on the Cu mesh structure. As shown in Fig. 6, the sheet resistance of the Cu mesh/PVA film-based TH exponentially dropped from ~ 10.9 ohnm/sq to ~ 8.9 Ω/sq (18.3% decresae) after self-annealing at ~ 85 ℃ for 3 h. The decrease in the sheet resistance is attributed to the increased electrical connectivity between the Cu particles after Joule heating (self-annealing) [35]. Hence, the sheet resistance of the Cu mesh/PVA film-based TH can be effectively reduced through the self-annealing process, thereby reducing the power consumption and improving the heat generation performance of the TH.

Figure 7, Additional file 1: Figures S5, and S6 show the operation of the Cu mesh/PVA film-based THs with various shapes and sizes. When the TH was attached to curved surfaces, such as a round-bottom flask and finger (see the Additional file 1: Figure S5 and S6, respectively), the TH retained its normal functions. In addition, the TH fixed on the back of the hand opreated normally when the fist was clenched and opened, as shown in the Fig. 7. These results indicate the applicability of the fabricated Cu mesh/PVA film-based TCF as a flexible/wearable TH.

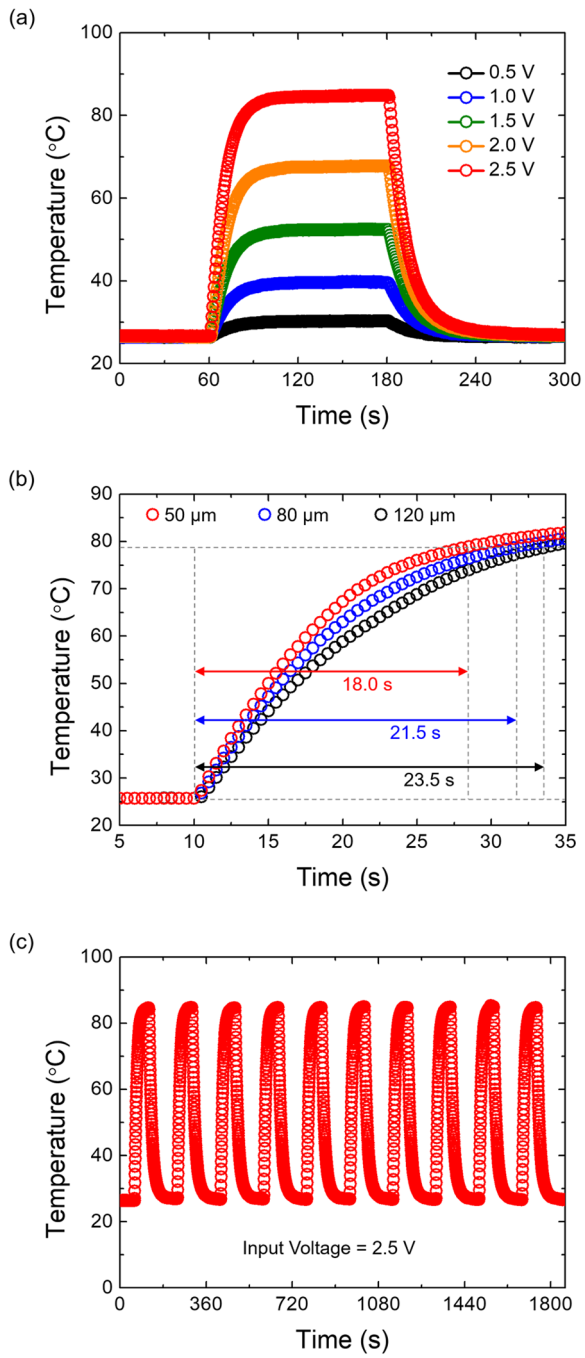

Fig. 5 **a** Heat generation performance of the Cu mesh/PVA film heater (20 mm × 20 mm) as a function of time at an applied voltage of 0.5, 1.0, 1.5, 2.0, and 2.5 V. **b** Time–temperature curves of the Cu mesh/PVA film TH of different PVA substrate thicknesses. The time provided in the graphs indicate the response time of the THs. **c** Results of the cyclic test of the heat generation of the Cu mesh/PVA film heater with an applied voltage of 2.5 V

Table 2 Comparison of the performances of the Cu mesh/PVA film heaters fabricated with various PVA film thicknesses

Thickness (μm)	R_s (ohm/sq)	Max. Temp. at 2.5 V (℃)	Response time (s)	Ramping rate (℃/s)
50	~11.0	84.7	18.0	2.94
80		84.5	21.5	2.46
120		84.4	23.5	2.25

Table 3 Changes in the performance of the Cu mesh/PVA film-based TH during the cyclic test

Cycle No	R_s (ohm/sq)	Max. Temp (℃)	Response time (s)	Min. Temp (℃)
0	11.0	–	–	–
1	10.8	84.6	18.0	26.9
2	10.8	84.7	18.0	26.7
3	10.9	84.5	17.5	26.8
4	10.8	84.7	18.0	26.7
5	10.8	84.8	18.5	26.8
6	10.8	84.9	18.5	26.8
7	10.9	84.8	18.0	26.7
8	11.0	84.9	18.5	26.8
9	10.8	84.9	18.5	26.9
10	10.9	84.6	18.0	26.8

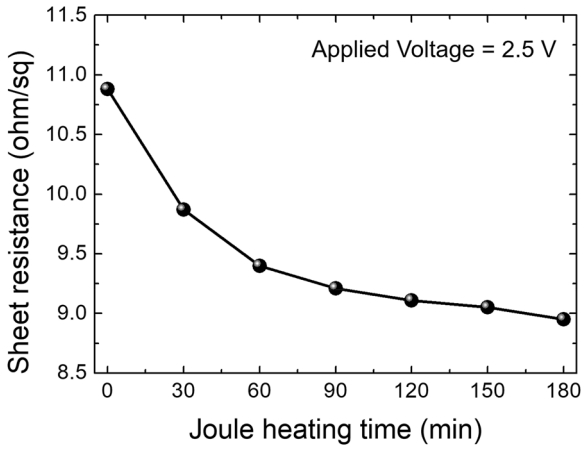

Fig. 6 Change in the sheet resistance of the Cu mesh/PVA film with respect to the thermal treatment time by Joule heating

Taken together, the proposed method has the advantage that there are no additional processing techniques such as lift-off, etching, or electroplating, compared with the previous studies on the fabrication of high-performance flexible/wearable THs [23, 30, 32, 35]. In addition, it was found that the thermal response time of

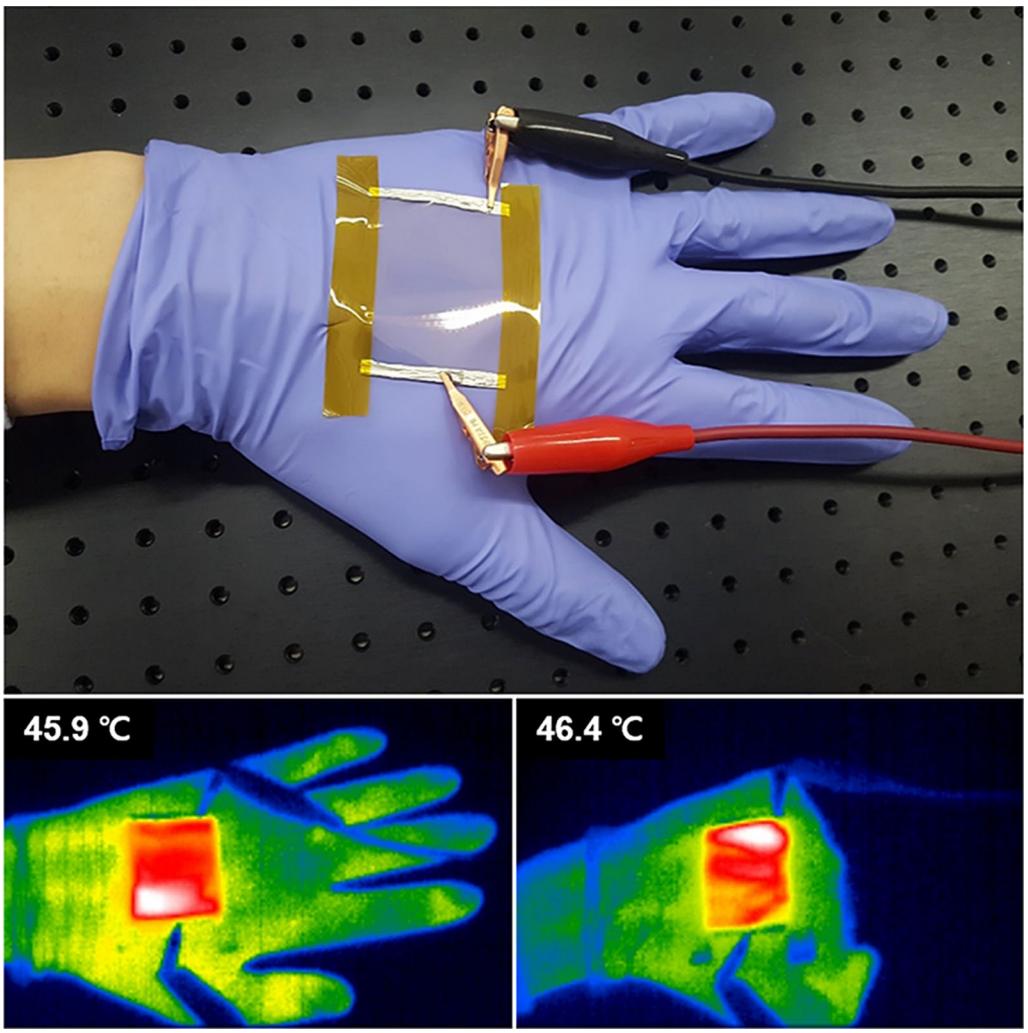

Fig. 7 Photograph and IR thermal images of the operation of the Cu mesh/PVA film-based TH (45 mm × 45 mm) attached to the back of the hand

the heater was shortened in proportion to the decrease in the thickness of the heater substrate.

Conclusion

In summary, we developed a lightweight flexible TCF by transfer printing a 100 nm thick Cu mesh structure onto PVA films of various thicknesses for application in wearable heaters. A Cu mesh-based lightweight TCF fabricated on a ~ 50 μm thick PVA substrate demonstrated optical and electrical properties comparable to those of commercial ITO glass. In addition, the Cu mesh/PVA film-based TCF exhibited superior mechanical flexibility compared to the ITO thin film sputtered on the same substrate. The TCF demonstrated its rapid Joule heating behavior with a response time of ~ 18.0 s and a ramping rate of ~ 3.0 ℃/s at a driving voltage of 2.5 V. The reliable response and recovery characteristics of the Cu mesh/PVA film-based TH were confirmed through the cyclic tests. Lastly, the lightweight TH attached to a human hand or round bottom flask successfully retained its normal functions. Based on the above research results, we expect that the Cu mesh-based lightweight TCF could be used as an ITO/FTO-free electrode/heater for advanced wearable electronic devices.

Abbreviations

TCF: Transparent conducting film; PVA: Poly(vinyl alcohol); TH: Transparent heater; TCO: Transparent conductive oxide; ITO: Indium tin oxide; FTO: Fluorine-doped tin oxide; PEDOT:PSS: Poly(3,4-ethylenedioxythiophene):poly(styrene sulfonate); NW: Nanowire; UV: Ultraviolet; PUA: Polyurethane acrylate; DC: Direct current; IR: Infrared; RT: Room temperature; LED: Light-emitting diode; FOM: Figure-of-merit; σ_{dc}: Electrical conductance; σ_{opt}: Optical conductance; R_S: Sheet resistance; T: Optical transmittance at 550 nm; Z_0: Impedance at free space; τ: Time constant; C: Heat capacity; h: Heat transfer coefficient; A: Surface area; c: Specific heat capacity; m: Mass; ρ: Density; d: Thickness film.

Supplementary Information

The online version contains supplementary material available at https://doi.org/10.1186/s40486-021-00132-5.

Additional file 1. Fabrication, optical and electrical properties, and heater performances of the Cu mesh/PVA film-based TCF.

Acknowledgements
This work was supported by the Technology Innovation Program (20006408) funded by the Ministry of Trade, Industry & Energy (MOTIE, Korea) and the Korea Innovation Foundation (INNOPOLIS) grant funded by the Korea government (MSIT) (2020-DD-UP-0278).

Authors' contributions
HK conducted the main experiment. YK supervised the project. All authors read and approved the final manuscript.

Funding
Technology Innovation Program (20006408).
Korea government (MSIT) (2020-DD-UP-0278).

Availability of data and materials
All data generated or analyzed during in this study are included in this published article and the supplementary information.

Declarations

Ethics approval and consent to participate
Not applicable.

Consent for publication
Not applicable.

Competing interests
The authors declare no competing interest (both financial and non-financial).

Received: 4 August 2021 Accepted: 14 October 2021
Published online: 25 October 2021

References

1. Patel M, Seo JH, Kim S et al (2021) Photovoltaic-driven transparent heater of ZnO-coated silver nanowire networks for self-functional remote power system. J Power Sources 491:229578. https://doi.org/10.1016/j.jpowsour.2021.229578
2. Huang WR, He Z, Wang JL et al (2019) Mass production of nanowire-Nylon flexible transparent smart windows for $PM_{2.5}$ capture. iScience 12:333–341. https://doi.org/10.1016/j.isci.2019.01.014
3. Kim HJ, Kim Y, Jeong JH et al (2015) A cupronickel-based micromesh film for use as a high-performance and low-voltage transparent heater. J. Mater. Chem. A 3:16621–16626. https://doi.org/10.1039/C5TA03348A
4. Veeramuthu L, Chen BY, Tsai CY et al (2019) Novel stretchable thermochromic transparent heaters designed for smart window defroster applications by spray coating silver nanowire. RSC Adv 9:35786–35796. https://doi.org/10.1039/C9RA06508C
5. Xie H, Cui K, Cui L et al (2020) H_2O-etchant-promoted synthesis of high-quality graphene on glass and its application in see-through thermochromic displays. Small 16:1905485. https://doi.org/10.1002/smll.201905485
6. Gueye MN, Carella A, Demadrille R et al (2017) All-polymeric flexible transparent heaters. ACS Appl Mater Interfaces 9:27250–27256. https://doi.org/10.1021/acsami.7b08578
7. Jo HS, An S, Kwon HJ et al (2020) Transparent body-attachable multifunctional pressure, thermal, and proximity sensor and heater. Sci Rep 10:2701. https://doi.org/10.1038/s41598-020-59450-0
8. Walia S, Gupta R, Rao KDM et al (2016) Transparent Pd wire network-based areal hydrogen sensor with inherent Joule heater. ACS Appl Mater Interfaces 8:23419–23424. https://doi.org/10.1021/acsami.6b08275
9. Kim HJ, Kim JH, Kim Y (2020) A fluoropolymer-coated nanometer-thick Cu mesh film for a robust and hydrophobic transparent heater. ACS Appl Nano Mater 9:8672–8678. https://doi.org/10.1021/acsanm.0c01404
10. Park J, Lee S, Kim DI et al (2019) Evaporation-rate control of water droplets on flexible transparent heater for sensor application. Sensors 19:4918. https://doi.org/10.3390/s19224918
11. Kim HJ, Choi DI, Lee S et al (2021) Quick thermal response-transparent-wearable heater based on copper mesh/poly(vinyl alcohol) film. Adv Eng Mater. https://doi.org/10.1002/adem.202100395
12. Park JW, Kang BH, Kim HJ (2020) A review of low-temperature solution-processed metal oxide thin-film transistors for flexible electronics. Adv Funct Mater 30:1904632. https://doi.org/10.1002/adfm.201904632
13. Bae JJ, Lim SC, Han GH et al (2012) Heat dissipation of transparent graphene defoggers. Adv Funct Mater 22:4819–4826. https://doi.org/10.1002/adfm.201201155
14. Kim Y, Lee HR, Saito T et al (2017) Ultra-thin and high-response transparent and flexible heater based on carbon nanotube film. Appl Phys Lett 110:153301. https://doi.org/10.1063/1.4978596
15. Kang TW, Kim SH, Kim CH et al (2017) Flexible polymer/metal/polymer and polymer/metal/inorganic trilayer transparent conducting thin film heaters with highly hydrophobic surface. ACS Appl Mater Interfaces 9:33129–33136. https://doi.org/10.1021/acsami.7b09837
16. Ji S, He W, Wang K et al (2014) Thermal response of transparent silver nanowire/PEDOT:PSS film heaters. Small 23:4951–4960. https://doi.org/10.1002/smll.201401690
17. Fan X, Nie W, Tsai H et al (2019) PEDOT:PSS for flexible and stretchable electronics: modifications, strategies, and applications. Adv Sci 6:1900813. https://doi.org/10.1002/advs.201900813
18. Zhu Z, Yang G, Li R et al (2017) Photopatternable PEDOT:PSS/PEG hybrid thin film with moisture stability and sensitivity. Microsyst Nanoeng 3:17004. https://doi.org/10.1038/micronano.2017.4
19. Wu J, Agrawal M, Becerril HA et al (2010) Organic light-emitting diodes on solution-processed graphene transparent electrodes. ACS Nano 4:43–48. https://doi.org/10.1021/nn900728d
20. Hong CH, Oh SK, Kim TK et al (2016) Electron beam irradiated silver nanowires for a highly transparent heater. Sci Rep 5:17716. https://doi.org/10.1038/srep17716
21. Jang J, Hyun BG, Ji S et al (2017) Rapid production of large-area, transparent and stretchable electrodes using metal nanofibers as wirelessly operated wearable heaters. NPG Asia Mater 9:e432. https://doi.org/10.1038/am.2017.172
22. Hong S, Lee H, Lee J et al (2015) Highly stretchable and transparent metal nanowire heater for wearable electronics applications. Adv Mater 27:4744–4751. https://doi.org/10.1002/adma.201500917
23. Chen X, Nie S, Guo W et al (2019) Printable high-aspect ratio and high-resolution Cu grid flexible transparent conductive film with figure of merit over 80000. Adv Electron Mater 5:1800991. https://doi.org/10.1002/aelm.201800991
24. Kim HJ, Lee SH, Lee J et al (2014) High-durable AgNi nanomesh film for a transparent conducting electrode. Small 10:3767–3774. https://doi.org/10.1002/smll.201400911
25. Zhang X, Yan X, Chen J et al (2014) Large-size graphene microsheets as a protective layer for transparent conductive silver nanowire film heaters. Carbon 69:437–443. https://doi.org/10.1016/j.carbon.2013.12.046
26. Lan W, Chen Y, Yang Z et al (2017) Ultraflexible transparent film heater made of Ag nanowire/PVA composite for rapid-response thermotherapy pads. ACS Appl Mater Interfaces 9(6644):6651. https://doi.org/10.1021/acsami.6b16853
27. Chen D, Fan G, Zhang H et al (2019) Efficient Ni/Au mesh transparent electrodes for ITO-free planar Perovskite solar cells. Nanomaterials 9:932. https://doi.org/10.3390/nano9070932
28. Ahn Y, Jeong Y, Lee Y (2012) Improved thermal oxidation stability of solution-processable silver nanowire transparent electrode by reduced graphene oxide. ACS Appl Mater Interfaces 4:6410–6414. https://doi.org/10.1021/am301913w
29. Song M, Kim HJ, Kim CS et al (2015) ITO-free highly bendable and efficient organic solar cells with Ag nanomesh/ZnO hybrid electrodes. J Mater Chem A 3:65–70. https://doi.org/10.1039/C4TA05294C

30. Chen X, Wu X, Shao S et al (2017) Hybrid printing metal-mesh transparent conductive films with lower energy photonically sintered copper/tin ink. Sci Rep 7:13239. https://doi.org/10.1038/s41598-017-13617-4
31. Wang S, Zhang X, Zhao W (2013) Flexible, transparent, and conductive film based on random networks of Ag nanowires. J Nanomater 2013:456098. https://doi.org/10.1155/2013/456098
32. Wu H, Kong D, Ruan Z et al (2013) A transparent electrode based on a metal nanothrough network. Nat Nanotechnol 8:421–425. https://doi.org/10.1038/nnano.2013.84
33. Tokuno T, Nogi M, Karakawa M et al (2011) Fabrication of silver nanowire transparent electrodes at room temperature. Nano Res 4:1215–1222. https://doi.org/10.1007/s12274-011-0172-3
34. Kim HJ, Song M, Jeong JH et al (2016) Highly efficient and stable cupronickel nanomesh electrode for flexible organic photovoltaic devices. J Power Sources 331:22–25. https://doi.org/10.1016/j.jpowsour.2016.09.024
35. Rao KDM, Kulkarni GU (2014) A highly crystalline single Au wire network as a high temperature transparent heater. Nanoscale 6:5645–5651. https://doi.org/10.1039/C4NR00869C
36. Nikzad MJ, Mohamadbeigi N, Sadrnezhaad SK et al (2019) Fabrication of a highly flexible and affordable transparent electrode by aligned U-shaped copper nanowires using a new electrospinning collector with convenient transferability. ACS Omega 4:21260–21266. https://doi.org/10.1021/acsomega.9b02760

Publisher's Note